

Reactivity of Permethylzirconocene and Permethyltitanocene toward Disubstituted 1,3-Butadiynes: η^4 - vs η^2 -Complexation or C–C Coupling with the Permethyltitanocene

Paul-Michael Pellny, Frank G. Kirchbauer, Vladimir V. Burlakov, Wolfgang Baumann, Anke Spannenberg, and Uwe Rosenthal*

Contribution from the Institut für Organische Katalyseforschung an der Universität Rostock e.V., Buchbinderstr. 5-6, D-18055 Rostock, Germany

Received April 1, 1999

Abstract: This paper describes the reactivity of permethylzirconocene and permethyltitanocene toward different 1,3-butadiynes. A pointed dependence on the metals and the diyne substituents was found. Unusual, but still stable, five-membered zirconacyclocumulenes (η^4 -diyne complexes, zirconacyclopenta-2,3,4-trienes) $\text{Cp}^*_2\text{Zr}(\eta^4\text{-}1,2,3,4\text{-RC}_4\text{R})$, R = Ph and SiMe_3 , were prepared using two new and effective synthetic routes. One starts with the permethylzirconocene bisacetylides $\text{Cp}^*_2\text{Zr}(\text{C}\equiv\text{CR})_2$, R = Ph (**1a**), SiMe_3 (**1b**), which rearrange in sunlight to form the stable five-membered zirconacyclocumulenes $\text{Cp}^*_2\text{Zr}(\eta^4\text{-}1,2,3,4\text{-RC}_4\text{R})$, R = Ph (**2a**), SiMe_3 (**2b**). The alternative route to **2a** and **2b** is the reduction of $\text{Cp}^*_2\text{ZrCl}_2$ with Mg in the presence of the adequate disubstituted butadiynes $\text{RC}\equiv\text{C}-\text{C}\equiv\text{CR}$. Both methods failed to produce the analogous titanacyclocumulenes, which seemed extremely unstable. Nevertheless, we were able to obtain distinct products employing the reduction pathway with permethyltitanocene. For R = SiMe_3 , the novel titanacyclocumulene (η^2 -complex) $\text{Cp}^*_2\text{Ti}(\eta^2\text{-}1,2\text{-Me}_3\text{SiC}_2\text{C}\equiv\text{CSiMe}_3)$ (**3**) was isolated. For R = Ph, an activation of both pentamethylcyclopentadienyl ligands was observed resulting in the complex $[\eta^5\text{-C}_5\text{Me}_4\text{-(CH}_2\text{)-Ti}(\text{-C(=CHPh)C(=CHPh)CH}_2\text{-}\eta^5\text{-C}_5\text{Me}_4)]$ (**4**). The reaction of **4** with carbon dioxide led to the Cp^* -substituted titanafuranone $\text{Cp}^*\text{Ti}[\text{-OC(=O)C(Ph)C(-)C(=CHPh)CH}_2\text{-}\eta^5\text{-C}_5\text{Me}_4]$ (**5**). The zirconacyclocumulene **2b** surprisingly inserted two molecules of CO_2 to give the unprecedented cumulenyl dicarboxylate $\text{Cp}^*_2\text{Zr}[\text{-OC(=O)C(SiMe}_3\text{)=C=C=C(SiMe}_3\text{)C(=O)O-}]$ (**6**). The η^2 -complex **3** (titanacyclocumulene) took up one molecule of carbon dioxide to afford the titanafuranone $\text{Cp}^*_2\text{Ti}[\text{OC(=O)C(SiMe}_3\text{)=C(C}\equiv\text{CSiMe}_3\text{)-}]$ (**7**).

Introduction

In modern acetylene chemistry,¹ synthesis of carbon rich compounds is an intensively researched area which is also directed toward organometallic polymers with conjugated π systems.² Such compounds often form the basis for high-grade materials in the field of material science.³ For the synthesis of various carbon networks,⁴ it is interesting to understand the principles of the coupling of polyynes $\text{R}(\text{C}\equiv\text{C})_2\text{R}$. Since these polyalkyne compounds are difficult to investigate, butadiynes $\text{R}(\text{C}\equiv\text{C})_n\text{R}$ as the smaller homologues were first used as model compounds, and there are a few relevant publications about interesting reactions of conjugated as well as of nonconjugated diynes with titanocene and zirconocene.⁵ Detailed investigations have been conducted by the authors into the reactions of differently substituted 1,3-butadiynes with the complexes

$\text{Cp}_2\text{M}(\text{L})(\eta^2\text{-Me}_3\text{SiC}_2\text{SiMe}_3)$ (M = Ti, L = -; M = Zr, L = THF, pyridine) as metallocene sources.^{5k} We often found unexpected results, e.g., different complexations, a C–C single bond cleavage and various types of coupling reactions. The generated products proved to be strongly dependent on the substituents R attached to the diynes, the metals M of the metallocenes, and the stoichiometries employed.^{5k}

The outstanding result of these studies was the discovery that the metallocenes “ Cp_2M ” (M = Ti, Zr)^{5k} react with $\text{tBuC}\equiv\text{C}-\text{C}\equiv\text{CtBu}$ to produce stable five-membered metallacyclocumulenes (η^4 -complexes, metallacyclopenta-2,3,4-trienes) $\text{Cp}_2\text{M}(\eta^4\text{-}1,2,3,4\text{-tBuC}_4\text{tBu})$, M = Zr,⁶ Ti.⁷ The X-ray diffraction studies of these complexes have shown the ring system to be planar and to contain three C–C double bonds from which the central bond is internally coordinated to the metal center. These structural features support the description of those compounds

(1) (a) Diederich, F. *Oligoacetylenes*. In *Modern Acetylene Chemistry*; Stang, P. J., Diederich, F., Eds.; VCH: Weinheim, 1995; p 443. (b) Diederich, F.; Rubin, Y. *Angew. Chem., Int. Ed. Engl.* **1992**, *31*, 1101. (c) Gleiter, R.; Kratz, D. *Angew. Chem., Int. Ed. Engl.* **1993**, *32*, 842.

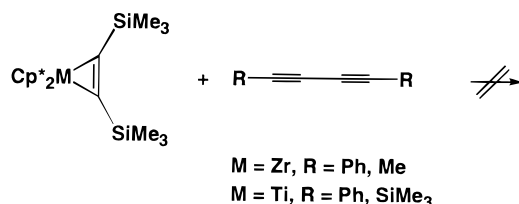
(2) (a) Beck, W.; Niemer, B.; Wieser, M. *Angew. Chem.* **1993**, *105*, 969; *Angew. Chem., Int. Ed. Engl.* **1993**, *32*, 923. (b) Altmann, M.; Bunz, U. H. F. *Angew. Chem., Int. Ed. Engl.* **1995**, *34*, 569. (c) Lang, H. *Angew. Chem., Int. Ed. Engl.* **1994**, *33*, 547. (d) Pirio, N.; Touchard, D.; Dixneuf, P. H.; Fettouhi, M.; Ouahab, L. *Angew. Chem., Int. Ed. Engl.* **1992**, *31*, 651. (e) Weng, W.; Bartik, T.; Brady, M.; Bartik, B.; Ramsden, A. M. A.; Gladysz, J. A. *J. Am. Chem. Soc.* **1995**, *117*, 7129. (f) Werner, H. *Nachr. Chem. Tech. Lab.* **1992**, *140*, 435.

(3) Skotheim, T. A. In *Handbook of Conductive Polymers*; M. Dekker: New York, 1986; Vols. 1 and 2.

(4) Bunz, U. *Angew. Chem., Int. Ed. Engl.* **1994**, *33*, 1127.

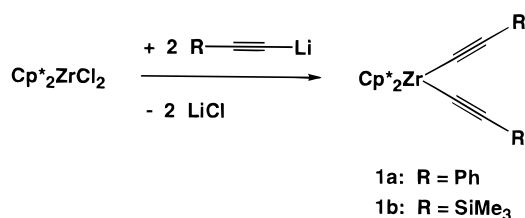
(5) (a) Nugent, W. A. Taber, D. F. *J. Am. Chem. Soc.* **1989**, *111*, 6435 and references therein. (b) Mao, S. S. H.; Tilley, T. D. *J. Am. Chem. Soc.* **1995**, *117*, 5365. (c) Mao, S. S. H.; Tilley, T. D. *J. Am. Chem. Soc.* **1995**, *117*, 7031. (d) Mao, S. S. H.; Liu, F.-Q.; Tilley, T. D. *J. Am. Chem. Soc.* **1998**, *120*, 1193. (e) Hsu, D. P.; Davis, W. M.; Buchwald, S. L. *J. Am. Chem. Soc.* **1993**, *115*, 10394. (f) Warner, B. P.; Davis, W. M.; Buchwald, S. L. *J. Am. Chem. Soc.* **1994**, *116*, 5471. (g) Du, B.; Faroni, M. F.; McConville, D. B.; Youngs, W. J. *Tetrahedron* **1995**, *51*, 4359. (h) Takahashi, T.; Aoyagi, K.; Denisov, V.; Suzuki, N.; Chouairy, D.; Negishi, E. *Tetrahedron Lett.* **1993**, *34*, 8301. (i) Takahashi, T.; Kasai, K.; Xi, Z.; Denisov, V. *Chem. Lett.* **1995**, 347. (j) Takahashi, T.; Xi, Z.; Obora, Y.; Suzuki, N. *J. Am. Chem. Soc.* **1995**, *117*, 2665. (k) Liu, F.-Q.; Harder, G.; Tilley, T. D. *J. Am. Chem. Soc.* **1998**, *120*, 3271. (l) Ohff, A.; Pulst, S.; Peulecke, N.; Arndt, P.; Burlakov, V. V.; Rosenthal, U. *Synlett* **1996**, 111 and references therein.

SiMe₃), M = Ti,²³ Zr,²⁵ in corresponding reactions, a clean substitution of the acetylene ligand by the diyne was not observed; the permethyltitanocene complex Cp*₂Ti(η²-Me₃SiC₂-SiMe₃)²³ did not react with PhC≡C-C≡CPh and Me₃SiC≡C-C≡CSiMe₃ in a reaction time of 5 days at room temperature (eq 2). The same outcome was found in the reaction of Cp*₂Zr(η²-Me₃SiC₂SiMe₃)²⁵ with PhC≡C-C≡CPh. When heating a mixture of Cp*₂Zr(η²-Me₃SiC₂SiMe₃) and MeC≡C-C≡CMe to 60 °C for 24 h, four hitherto unidentified complexes were indicated, however, next to almost 80% of the starting material (eq 2).



An explanation for the unsuccessful reactions can be deduced from the mechanism of the substitution of the bis(trimethylsilyl)acetylene by ethylene in Cp₂Zr(THF)(η²-Me₃SiC₂SiMe₃). For this reaction path, an associative mechanism has been described (commencing addition of ethylene and subsequent elimination of silylacetylene).²⁶ It is assumed that the steric restrictions resulting from the bulky permethylcyclopentadienyl ligands minimize the likelihood of bimolecular reactions and prevent similar conversions with the diynes in the examples mentioned above.

The reaction pathway employed for the preparation of the Cp-coordinated metallacyclocumulenes could not be adapted to establish metallacyclocumulenes with pentamethylcyclopentadienyl ligands. A new synthetic route to the Cp* analogues had to be designed. In our studies on the reactions of Cp₂Ti(C≡C^tBu)₂ upon irradiation, we discovered the intermediacy of the titanacyclocumulene Cp₂Ti(η⁴-1,2,3,4-^tBuC₄tBu) (as monitored by NMR measurements). However, we were not able to isolate this complex, as it readily reacted with free "Cp₂Ti" to yield dimeric complexes.¹² The detection of such an intermediate in that reaction led to the establishment of a procedure to prepare five-membered permethylzirconacyclocumulenes in significant quantities. It starts with the new permethylmetallocene bisacetylides Cp*₂Zr(C≡CR)₂, R = Ph (**1a**), SiMe₃ (**1b**). They are prepared by a salt elimination reaction starting from the complex Cp*₂ZrCl₂ and 2 equiv of the corresponding acetylides RC≡CLi (eq 3). Different solvents, e.g., THF, toluene, and diethyl ether, have been examined in these conversions, and toluene proved to provide the best yields, although these still have to be considered poor (22% and 37%).



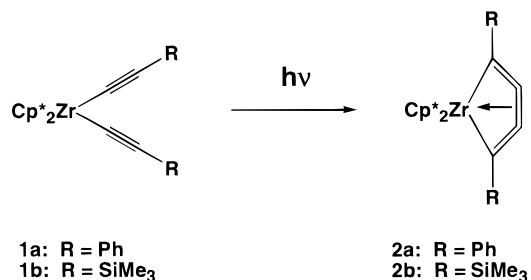
The rearrangement of these permethylzirconocene bisacetylides Cp*₂Zr(C≡CR)₂ **1a** and **1b** in sunlight affords the complexes

(20) (a) Strauss, I. Ph.D. Thesis, RWTH Aachen, 1997. (b) Beckhaus, R.; Strauss, I.; Wagner, T. Unpublished results.

(21) Beckhaus, R.; Sang, J.; Oster, J.; Wagner, T. *J. Organomet. Chem.* **1994**, *484*, 179.

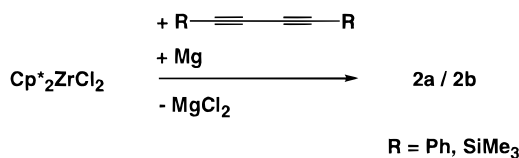
(22) Carney, M. J.; Walsh, P. J.; Hollander, F. J.; Bergman, R. G. *J. Am. Chem. Soc.* **1989**, *111*, 8751.

Cp*₂Zr(η⁴-1,2,3,4-RC₄R), R = Ph (**2a**), SiMe₃ (**2b**), (eq 4).



Of special note is that the observed rearrangement confirms the result of theoretical calculations stating that the metallacyclocumulenes are thermodynamically more stable than the bisacetylide complexes.^{9a} A reaction similar to this rearrangement has previously been postulated^{8a} and later realized in the Lewis acid-catalyzed conversion of Cp₂Zr(C≡CMe)₂.^{8b}

As an alternative to the photocatalyzed reaction, the reduction of Cp*₂ZrCl₂ in THF with magnesium in the presence of the butadiynes PhC≡C-C≡CPh or Me₃SiC≡C-C≡CSiMe₃ was established as an elegant and effective procedure to obtain the complexes **2a** and **2b** in a direct way (eq 5).



The second method (eq 5) can be regarded as more general and starts with simpler substrates, although better yields were obtained by the rearrangement of the permethylzirconocene bisacetylides Cp*₂Zr(C≡CR)₂ in sunlight (eq 4).

The new zirconacyclocumulenes with pentamethylcyclopentadienyl ligands Cp*₂Zr(η⁴-1,2,3,4-RC₄R), R = Ph (**2a**), SiMe₃ (**2b**), show ¹³C NMR signals [**2a**: 118.4 (C-β), 179.4 (C-α). **2b**: 144.5 (C-β), 188.0 (C-α)] in a typical region also found for the unsubstituted cyclopentadienyl complexes Cp₂M(η⁴-1,2,3,4-RC₄R) [M = Ti, R = Ph: 103.1 (C-β), 176.8 (C-α).¹¹ M = Ti, R = ^tBu: 94.7 (C-β), 181.9 (C-α)⁷, M = Zr, R = ^tBu: 105.5 (C-β), 186.4 (C-α)⁶]. As a result of the special bonding situation,^{6,7,9a} the shifts of the β carbon atoms are smaller than expected for typical (linear) cumulene systems. A small influence of the metal and a somewhat stronger effect of the substituents is noteworthy; zirconium and silyl substituents cause a low-field shift of the carbon atom in the β position. This tendency has also been documented for alkyne complexes.

The zirconacyclocumulenes **2a** and **2b** were investigated by X-ray crystal structure analyses. The molecular structures are shown in Figures 1 and 2. The structures of the permethylmetallocene complexes **2a** and **2b** are similar to the formerly described corresponding five-membered metallacyclocumulenes of Cp₂M (see Table 1), which explicitly differ from metallacyclopentadienes. Table 1 presents the relevant bond distances and angles. The four carbon atoms of the former butadiyne unit and the Zr atom form a planar arrangement. The three C-C

(23) Burlakov, V. V.; Polyakov, A. V.; Yanovsky, A. I.; Struchkov, Y. T.; Shur, V. B.; Vol'pin, M. E.; Rosenthal, U.; Görls, H. *J. Organomet. Chem.* **1994**, *476*, 197.

(24) Rosenthal, U.; Ohff, A.; Michalik, M.; Görls, H.; Burlakov, V. V.; Shur, V. B. *Angew. Chem., Int. Ed. Engl.* **1993**, *32*, 1193.

(25) Hiller, J.; Thewalt, U.; Polasek, M.; Petrusova, L.; Varga, V.; Sedmera, P.; Mach, K. *Organometallics* **1996**, *15*, 3752.

(26) Mansel, S.; Thomas, D.; Lefebvre, C.; Heller, D.; Kempe, R.; Baumann, W.; Rosenthal, U. *Organometallics* **1997**, *16*, 2886.

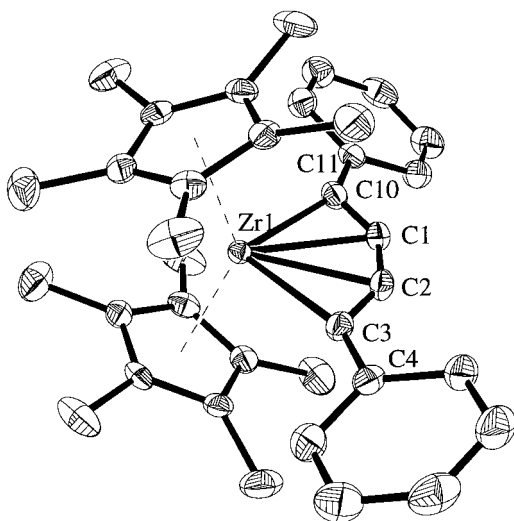


Figure 1. ORTEP diagram (30% probability) of complex **2a**. Selected bond distances (Å) and angles (deg): C1–C10 1.305(5), C1–C2 1.327(4), C2–C3 1.296(5), Zr1–C10 2.345(4), Zr1–C1 2.328(4), Zr1–C2 2.330(4), Zr1–C3 2.357(4), C10–Zr–C3 97.63(11), C11–C10–C1 133.0(3), C10–C1–C2 148.0(4), C1–C2–C3 148.5(4), C2–C3–C4 134.3(4).

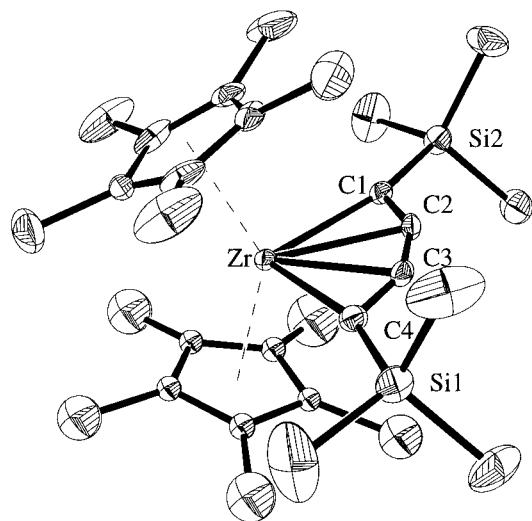


Figure 2. ORTEP diagram (30% probability) of complex **2b**. The disordered groups (one Cp* ring) have been omitted for clarity. Selected bond distances (Å) and angles (deg): C1–C2 1.291(6), C2–C3 1.337(6), C3–C4 1.293(6), Zr–C1 2.422(4), Zr–C2 2.305(4), Zr–C3 2.307(4), Zr–C4 2.426(5), C1–Zr–C4 96.85(15), Si2–C1–C2 163.1(3), C1–C2–C3 152.5(4), C2–C3–C4 152.3(4), C3–C4–Si1 128.4(3).

bond lengths [**2a**: 1.296(5), 1.327(4), 1.305(5). **2b**: 1.291(6), 1.337(6), 1.293(6) Å] indicate that these bonds are of roughly similar bond order, displaying double bond character. All four carbon atoms of the ring have p orbitals perpendicular to the plane of the cyclopentadiene. The sp-hybridized internal C atoms possess additional p orbitals in that plane. Employing these orbitals, the central C–C double bond is coordinated to the metal center, resulting in an elongated C–C double bond. In accordance with this description the M–(C-β) distances [**2a**: 2.328(4), 2.330(4). **2b**: 2.305(4), 2.307(4)] are shorter than the M–(C-α) bonds [**2a**: 2.345(4), 2.357(4); **2b**: 2.422(4), 2.426(5) Å]. An informative view of **2a** is that parallel to the plane Zr–C1–C2–C3–C10, which shows the phenyl rings in a minimum of steric interactions; they are tilted slightly out of that plane [22.9° and 25.3°] displaying an angle of 48.2° between them. Both are nearly parallel to the plane of one of the Cp*

Table 1. Structural Data of Five-Membered Metallacyclocumulenes L₂M(η⁴-1,2,3,4-RC₄R)

L/M/R	Cp/Ti ⁺ /Bu ³	Cp/Zr ⁺ /Bu ²	Cp*/Zr/Ph (2a)	Cp*/Zr/SiMe ₃ (2b)
distances (Å)				
M–Cα	2.252(9)	2.357(5)	2.345(4)	2.422(4)
M–Cα′	2.298(10)	2.307(5)	2.357(4)	2.426(5)
M–Cβ	2.209(9)	2.303(5)	2.328(4)	2.305(4)
M–Cβ′	2.213(9)	2.306(5)	2.330(4)	2.307(4)
Cα–Cβ	1.243(13)	1.28(1)	1.296(4)	1.291(6)
Cβ–Cβ′	1.339(13)	1.31(1)	1.327(4)	1.337(6)
Cα′–Cβ′	1.276(11)	1.29(1)	1.305(5)	1.293(6)
angles (deg)				
M–Cα–Cβ	70.3(6)	73.7(3)	72.8(2)	69.2(3)
M–Cα′–Cβ′	71.6(6)	71.7(3)	73.1(2)	69.2(3)
M–Cα–R	138.1(9)	151.3(4)	152.4(3)	163.1(3)
M–Cα′–R	139.2(10)	151.1(4)	153.2(3)	162.4(3)
Cα–Cβ–Cβ′	150.0(10)	150.0(10)	148.5(4)	152.5(4)
Cα′–Cβ′–Cβ	147.8(10)	147.2(5)	148.0(4)	152.3(4)
Cα–M–Cα′	100.4(4)	97.4(2)	97.63(11)	96.85(15)
L–M–L	129.7	129.7	137.3	135.7/137.1

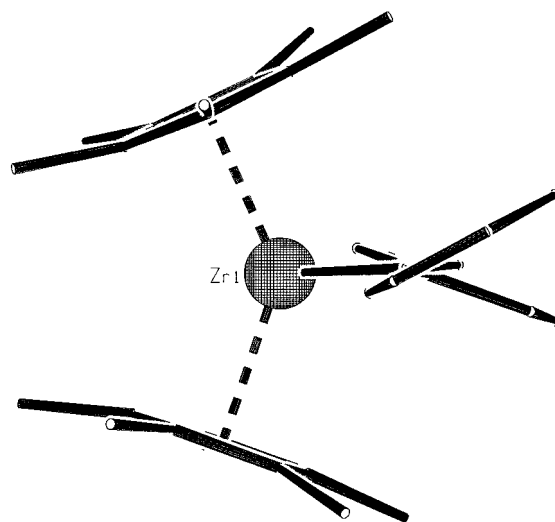


Figure 3. Perspective view of complex **2a** parallel to the plane Zr–C1–C2–C3–C10.

ligands [deviations of 1.7° and 4.5°] and inclined to the obverse other one [47.1° and 44.8°] (Figure 3). The angle between the centroids of the Cp* ligands about the metal is 137.3°.

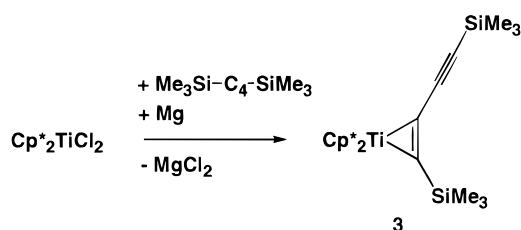
As a result of the three-dimensional structure of the trimethylsilyl substituent, a comparatively clear view and quantifying analysis cannot be presented for **2b**. Nevertheless, it is our conviction that **2b** presents us with the more interesting structure. The large permethylzirconocene unit does not prevent the access of the demandingly substituted butadiyne. Despite emphasized steric crowding, the formation of the fairly stable **2b** was successful.

All four metallacyclocumulenes described in Table 1 exhibit very uniform structural features and thus prove a marginal influence of the metals, the Cp*(*) ligands, and the substituents of the diynes on the bond distances and angles.

Reduction of Cp*₂TiCl₂ with Magnesium in the Presence of 1,3-Butadiynes: Synthesis of a Titanacyclopentene (η²-Complex) and Two Different C–C Coupling Reactions of Permethyltitanocene. Both of the described preparative methods for zirconacyclocumulenes **2a** and **2b** failed to produce the corresponding Cp*-substituted titanacyclocumulenes. The irradiation of the permethyltitanocene bis(trimethylsilyl)acetylide produced complex **3** (63% yield).²⁷ The reduction of Cp*₂-TiCl₂ in the presence of RC≡C–C≡CR also failed to generate

the cumulene structure, but here we were able to isolate well-defined products.

The reaction with $\text{Me}_3\text{SiC}\equiv\text{C}-\text{C}\equiv\text{CSiMe}_3$ yielded the titanacyclopropene (η^2 -complex) $\text{Cp}^*_2\text{Ti}(\eta^2-1,2-\text{Me}_3\text{SiC}_2\text{C}\equiv\text{CSiMe}_3)$ (**3**), the first η^2 -butadiyne-titanocene complex ever described (eq 6).



This outcome was surprising as it manifested for the first time a structural type which was previously claimed as an intermediate in reactions of titanocenes “ Cp_2M ” with butadiynes. The only isolable products of these conversions of “ Cp_2Ti ” and butadiynes have been, depending on the stoichiometry, coupled and cleaved complexes, next to two titanacyclocumulenes.^{5k,7,11}

In this context, it is of special interest what Mach and co-workers reported in a recent paper: the system of $\text{Cp}^*_2\text{TiCl}_2$, $\text{Me}_3\text{SiC}\equiv\text{C}-\text{C}\equiv\text{CSiMe}_3$, and an excess of magnesium proceeded via a cleavage of the central C–C single bond of the diyne to afford a tweezer-like compound $[\text{Cp}^*_2\text{Ti}(\text{C}\equiv\text{CSiMe}_3)_2][\text{MgCl}(\text{THF})]$.²⁸ The stoichiometric use of Mg in this case led to a very different product.

The NMR spectroscopic behavior of $\text{Cp}^*_2\text{Ti}(\eta^2-\text{Me}_3\text{SiC}_2\text{C}\equiv\text{CSiMe}_3)$ (**3**) is clearly different from that of the η^4 -butadiyne complexes (metallacyclocumulenes such as **2a** and **2b**). At room temperature, no signals for the quaternary carbon atoms can be detected. The assumption of a dynamic behavior, deduced from the broad trimethylsilyl resonance, is confirmed upon cooling the sample. At 188 K (in toluene- d_8), two signals of equal intensity are found in the silyl region besides four resonances for quaternary carbon atoms. Two of them appear in the region characteristic of coordinated C–C triple bonds (205.3 and 227.5 ppm), the other two represent a free silyl-substituted C–C triple bond (105.1 and 110.7 ppm). The different character of the two unsaturated functionalities is also obvious from their IR absorptions (1608 and 2092 cm^{-1} , respectively). Consequently, two ^{29}Si NMR signals appear at -12.6 and -20.4 ppm (silicon at free triple bond, compare -19.3 ppm for $\text{Me}_3\text{SiC}\equiv\text{CSiMe}_3$).

The coalescence of the discussed signals (the Cp* resonances are not affected by the exchange process) is best explained by an interchanging coordination of the two triple bonds to the titanium center (Scheme 1). This would account for the apparent equivalence of the silyl groups at room temperature. The intermediacy of a metallacyclocumulene in this process is not proven, but most likely, for only the special combination of bulky C_5Me_5 and SiMe_3 groups around the small titanium atom seems to destabilize this species so that an alkyne complex (metallacyclopropene) is formed instead. A rough estimation of the activation barrier for this rearrangement (from $T_c = 217$ K and $\Delta\nu = 24$ Hz for the proton silyl signals) gives $\Delta G^\ddagger = 45$ kJ mol^{-1} .

Unfortunately, the averaged signals of the quaternary carbon atoms were not detected (decomposition took place before reaching the region of fast exchange). But the expected values

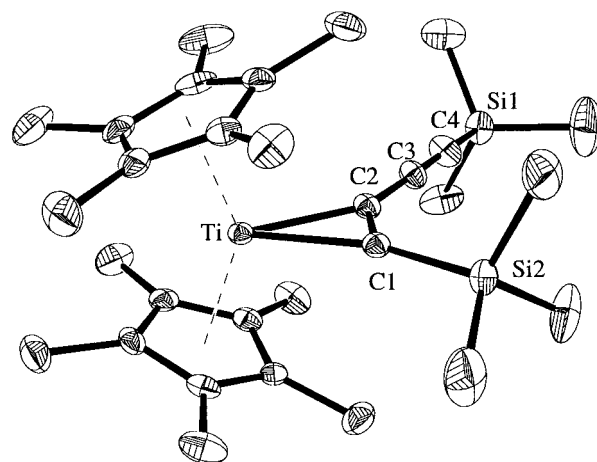
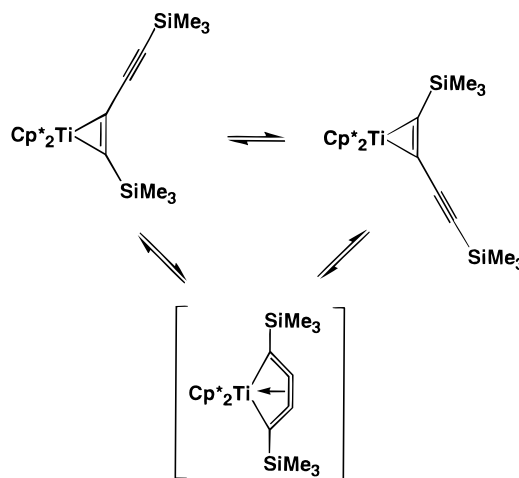


Figure 4. ORTEP diagram (30% probability) of complex **3**. Selected bond distances (Å) and angles (deg): C1–C2 1.311(4), Ti–C1 2.123(3), Ti–C2 2.085(3), C2–C3 1.401(4), C3–C4 1.215(4), C1–Ti–C2 36.30(10), Si2–C1–C2 130.0(2), C1–C2–C3 141.9(3), C2–C3–C4 174.7(3), C3–C4–Si1 171.7(3).

Scheme 1



(169.1 ppm for the silyl-substituted and 155.2 ppm for the central C atoms) clearly differ from those determined for metallacyclocumulenes (e.g., **2b** as the closest relative; see above: 188.0 and 144.5 ppm, respectively) and make clear that the symmetry found for the latter in solution results from their true constitution and not from a fast exchange as depicted in Scheme 1.

The permethyltitanocene η^2 -complex (metallacyclopropene) $\text{Cp}^*_2\text{Ti}(\eta^2-1,2-\text{Me}_3\text{SiC}_2\text{C}\equiv\text{CSiMe}_3)$ (**3**) was also analyzed by X-ray crystallography. An ORTEP drawing of **3** is shown in Figure 4. The structure of **3** represents the first example of a titanocene η^2 -complex with a 1,3-butadiyne. This bonding description is unequivocally proven by the detected bond lengths and angles. The data of the titanacyclopropene moiety are in the expected range. The distances [Ti–C1 2.123(3), Ti–C2 2.085(3), C1–C2 1.311(4) Å] are similar to those found in the well-known alkyne complexes $\text{Cp}^*_2\text{Ti}(\eta^2-\text{Me}_3\text{SiC}_2\text{SiMe}_3)$ ²³ [2.112(3), 2.126(3), 1.309(4) Å] and $\text{Cp}^*_2\text{Ti}(\eta^2-\text{PhC}_2\text{SiMe}_3)$ ²³ [2.098(2), 2.139(2), 1.308(3) Å]. The titanocene is characteristically bent showing a typical bite angle [141.4°]. The terminal alkyne's only weak deviation from linearity [C2–C3–C4 174.7(3)°, C3–C4–Si1 171.7(3)°] indicates that there is no interaction between this triple bond and the metal center. The length of the triple bond [C3–C4 1.215(4) Å] is as anticipated for alkynylsilanes.

(27) (a) Kirchbauer, F. G.; Ph.D. Thesis, University of Rostock, 1999. (b) Pellny, P.-M.; Kirchbauer, F. G.; Burlakov, V. V.; Baumann, W.; Spannenberg, A.; Rosenthal, U. *Chem. Eur. J.* **1999**, In press.

(28) Troyanov, S. I.; Varga, V.; Mach, K. *Organometallics* **1993**, *12*, 2820.

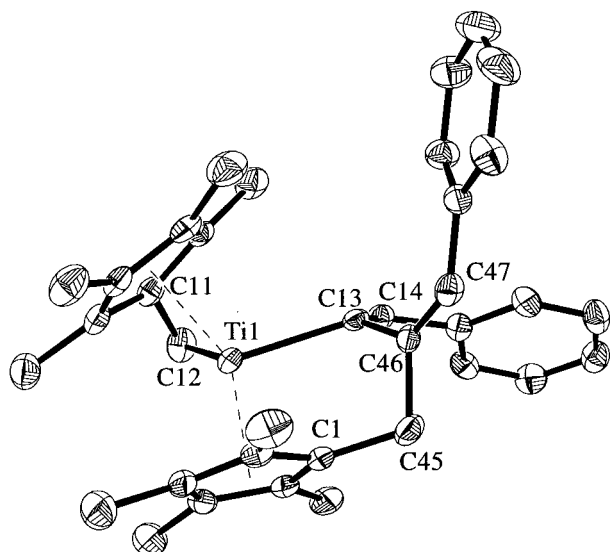
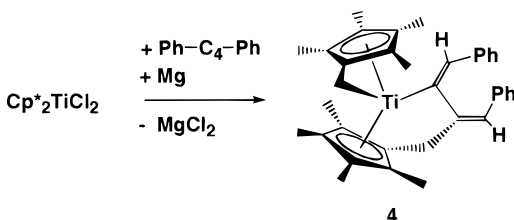


Figure 5. ORTEP diagram (30% probability) of complex **4**. Selected bond distances (Å) and angles (deg): C1–C45 1.513(6), C45–C46 1.525(6), C46–C47 1.357(6), C46–C13 1.467(6), C13–C14 1.322(6), C13–Ti1 2.246(4), C11–C12 1.444(6), C12–Ti1 2.271(5), C1–C45–C46 107.6(4), C45–C46–C47 120.4(4), C47–C46–C13 131.1(4), C46–C13–C14 123.9(4), C14–C13–Ti1 119.4(3), C11–C12–Ti1 66.4(3).

Using $\text{PhC}\equiv\text{C}-\text{C}\equiv\text{CPh}$ instead the reduction proceeds via an activation of both pentamethylcyclopentadienyl ligands leading to a coupling of one Cp^* ligand to the substrate and resulting in the complex $[\eta^5\text{-C}_5\text{Me}_4\text{-(CH}_2\text{)-}]\text{Ti}[\text{-C(=CHPh)C(=CHPh)CH}_2\text{-}\eta^5\text{-C}_5\text{Me}_4]$ (**4**) (eq 7).



The most prominent feature in the NMR spectra of complex **4** is the presence of eight singlets of equal intensity, representing eight different Cp^* methyl groups. Application of chemical shift correlation and NOE methods allows complete analysis and assignment of the ^1H and ^{13}C NMR spectra (for the labeling of the C atoms in **4** see Figures 5 and 9). The NOE cross-peaks are compatible with the solid-state structure of **4** (see below) without exception so that there is no doubt it is maintained in solution. The two-fold C–H activation in the permethyltitanocene moiety generates two functionally different cyclopentadienyl systems exhibiting, besides the mentioned methyl singlets, characteristic NMR properties.

C12, one of the methylene groups, is found at 79.5 ppm, dramatically low-field shifted relative to the other methyl groups. This shift indicates, together with the coupling constants $^1J(\text{C},\text{H})$ of 150 Hz and the small geminal coupling of the two protons (4.4 Hz), an increased *s* character. Hence, the description of this Cp^* system as a fulvene ligand is justified, even if the coordination of the exocyclic double bond is of strong metal-lacyclopropane character. The NMR data for the methylene group of the other cyclopentadienyl ligand are, however, not exceptional, a geminal H,H coupling of 13.5 Hz and $^1J(\text{C},\text{H})$ of 130 Hz show that C45 has to be described as an sp^3 hybridized carbon atom. Several long-range couplings, $^3J(\text{C45},-$

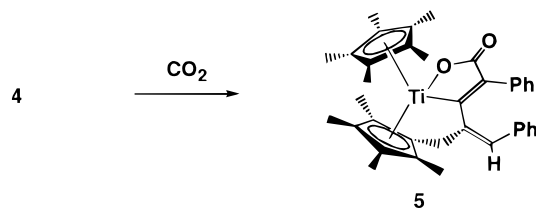
47-H) = 8 Hz or $^4J(\text{45-H},47\text{-H}) = 1.8$ Hz for instance, prove the coupling of the former butadiyne with the pentamethylcyclopentadienyl group.

The 1,3-butadiene system resulting from the two-fold hydrogen transfer onto the 1,3-butadiyne exhibits the characteristic ^{13}C NMR shift pattern, although it is strongly distorted from a planar conformation which is usually preferred. The central carbon atoms appear low-field shifted from the terminal ones, with an extreme shift (208.0 ppm) for C13 due to its metalation.

Figure 5 shows the molecular structure of the ligand-to-substrate coupled complex **4** as determined by an X-ray crystal structure analysis. The molecular structure of complex **4** proves the coupling of the butadiyne with one permethylcyclopentadienyl ring under the formation of a functionalized Cp^* ligand. The other Cp^* ring shows an activation of a methyl group resulting in the formation of a tetramethylfulvene ligand.¹⁹ The determined bond lengths are in the expected range for a $\pi\text{-}\eta^5\text{:}\sigma\text{-}\eta^1\text{-tetramethylfulvene}$ ligand [**4**: Ti1–C12 2.271(5), C11–C12 1.444(6) Å] as shown by a comparison to those found in the complex Cp^*FvTi [2.281(14), 1.437(14) Å].¹⁹ The metal–carbon distance for the functionalized Cp^* ligand [**4**: Ti–C13 2.246(4) Å] is typical for Ti–C(alkyl) bonds. The other bond distances in the chelating group are those of normal C–C single bonds [**4**: C13–C46 1.467(6), C45–C46 1.525(6), C1–C45 1.513(6) Å]. The exocyclic distances [**4**: C13–C14 1.322(6), C46–C47 1.357(6) Å] reflect C–C double bonds. This suggests a description of the substrate as a doubly fused 1,3-butadiene. The orientation of the phenyl groups minimizes steric repulsion between the substituents.

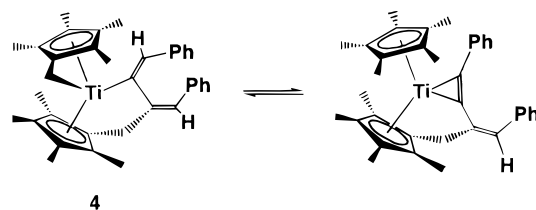
Reactions of 2a, 2b, 3, and 4 with Carbon Dioxide. These reactions with carbon dioxide epitomize the different reactivity of the obtained complexes.

The reaction of **4** with carbon dioxide in *n*-hexane generates the Cp^* -substituted titanafuranone $\text{Cp}^*\text{Ti}[\text{-OC(=O)C(Ph)-C(-)C(=CHPh)CH}_2\text{-}\eta^5\text{-C}_5\text{Me}_4]$ (**5**) (eq 8).



To explain the route by which **5** is formed, it seems reasonable to invoke the intermediacy of an isomeric η^2 -alkyne complex where the CO_2 inserts in. The formation of this proposed intermediate can be rationalized by a simple shift of one proton (Scheme 2). Such an intermediate would provide a plausible explanation of why complex **4** reacts with carbon dioxide in a similar manner as η^2 -alkyne complexes do.

Scheme 2



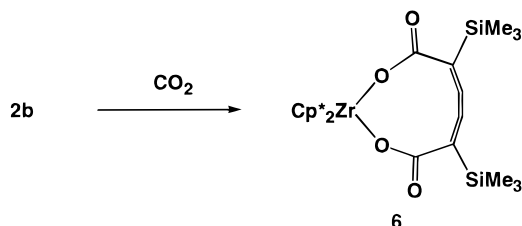
Evidence for the equilibrium proposed in Scheme 2 comes from the proton NMR spectrum of the starting complex **4**. A small amount (less than 5%) of a species with one intact $\text{C}_5\text{-Me}_5$ ligand (1.67 ppm, 15H) and one cyclopentadienyl system

linked to another fragment [four singlets, 3H each: 0.98, 1.10, 1.72, 2.00 ppm. CH₂ group: 3.52 ppm (d, 1H) and 3.99 ppm (dd, 1H), olef. CH: 5.55 ppm (br, 1H)] is present which may be regarded responsible for the formation of **5**, which itself exhibits a very similar shift pattern in its proton resonance spectrum.

The NMR spectra of **5** were analyzed in the same way as for complex **4**, they also prove that the solid-state structure is maintained in solution. The chemical shifts (see Experimental section) take the expected values (for other titanafuranones see ref 29 and references therein).

The structure of complex **5** (Figure 6) as a result of an addition of carbon dioxide to complex **4** shows the first Cp^{*}-substituted titanafuranone. It represents, in contrast to the parent fulvene complex **4**, a characteristically bent metallocene complex. Distances between the metal and the ring centers are 2.115 and 2.073 Å. The bite angle about the titanium center is 140.5°. These data are in good agreement with those of formerly described titanocenes. The Cp^{*}-substituted titanafuranone is characterized by typical bond distances in the metallacycle [5: Ti–C7 2.158(5), C7–C8 1.351(6), C8–C21 1.493(7), C21–O1 1.328(6), Ti–O1 1.943(3) Å]. These can be compared to those of the coupling product of toluene and carbon dioxide at a titanocene center [2.201(4), 1.340(5), 1.489(5), 1.327(5), 1.965(3) Å].^{29a} Two C–C single bonds form the bridge between the metallacycle and the Cp^{*} ligand as confirmed by the corresponding bond distances [C7–C23 1.477(6), C23–C24 1.541(6) Å]. A benzylidene group is attached to C23 [C23–C30 1.342(6) Å], which remains nearly unchanged from the one found in **4**.

Surprisingly the five-membered zirconacyclocumulene **2b** (η^4 -complex, zirconacyclopenta-2,3,4-triene), dissolved in THF, inserts two molecules of carbon dioxide to give the cumulenic dicarboxylate Cp^{*}₂Zr[OC(=O)C(SiMe₃)=C=C=C(SiMe₃)-C(=O)O-] (**6**) (eq 9).



The ¹H NMR spectrum displays only two singlets (0.20 and 1.90 ppm, relative ratio 9:15), indicating a symmetric molecule with equivalent silyl and cyclopentadienyl groups containing one butadiyne-derived fragment per zirconium. In the ¹³C NMR spectrum, three types of quaternary carbon atoms are found besides the silyl and cyclopentadienyl signals, the silylated carbon (134.4 ppm), the carbonyl group (167.8 ppm), and another low-field signal (185.9 ppm) which is characteristic for sp carbons in cumulenic hydrocarbons. A coordination of this butatriene system to zirconium cannot be deduced from these chemical shift data.

The structure of complex **6** as a result of the insertion of two molecules of carbon dioxide into complex **2b** is shown in Figure 7. It displays the first cumulenic dicarboxylate. The molecular structure reveals a characteristically bent metallocene arrangement of the ligands around zirconium. Distances between the

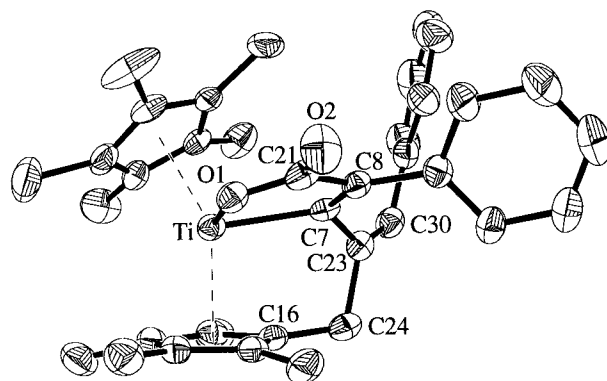


Figure 6. ORTEP diagram (30% probability) of complex **5**. Selected bond distances (Å) and angles (deg): Ti–C7 2.158(5), C7–C8 1.351(6), C8–C21 1.493(7), C21–O1 1.328(6), Ti–O1 1.943(3), C7–C23 1.477(6), C23–C24 1.541(6), C23–C30 1.342(6), C16–C24 1.508(7), C7–Ti–O1 78.2(2), Ti–O1–C21 120.6(3), O1–C21–C8 114.3(5), C21–C8–C7 114.0(5), C8–C7–Ti 112.6(4), C8–C7–C23 126.4(5), C7–C23–C30 134.2(5), C7–C23–C24 105.7(4), C16–C24–C23 109.0(4), C30–C23–C24 119.5(5).

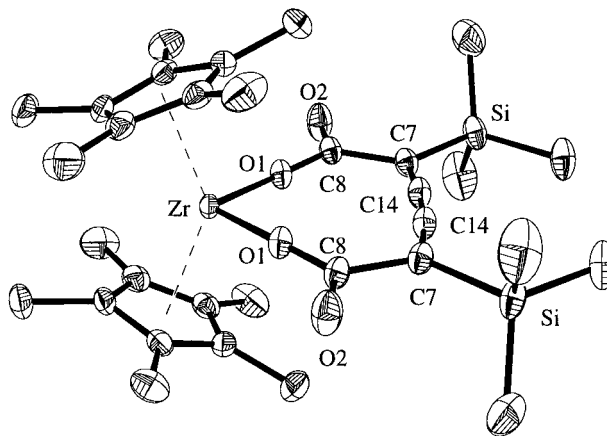


Figure 7. ORTEP diagram (30% probability) of complex **6**. Selected bond distances (Å) and angles (deg): Zr–O1 2.548(3), O1–C8 1.298(3), C8–C7 1.517(4), C7–Si 1.888(3), C7–C14 1.328(4), C14–C14 1.268(6), O1–Zr–O1 102.30(10), Zr–O1–C8 169.6(2), O1–C8–C7 116.6(2), C8–C7–C14 116.8(2), C8–C7–Si 118.4(2), Si–C7–C14 124.7(2), C7–C14–C14 173.1(2).

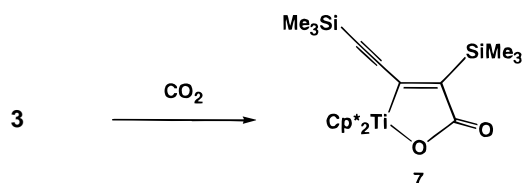
metal and both ring centers are 2.249 Å, the bite angle is 138.1°. These data are in good agreement with those of previously described zirconocenes. The most interesting structural feature of this nine-membered, monomeric metallacycle is the cumulenic C₄ unit. Three double bonds [1.328(4), 1.268(6), 1.328(4) Å] are found in an almost linear arrangement [173.1(2)°, 173.1(2)°]. The negligible deviation from linearity is due to the ring strain which is slightly mitigated by the hinted bending. The large distances between the metal center and the C₄ unit indicate that there is no coordination of this cumulene to the metal. The central C–C double bond displays a considerably shortened distance as compared to the outer bonds of the cumulene unit. This is an inversion of the ratios found in the five-membered metallacyclocumulenes where an elongated central double bond was determined. This can be explained by the fact that there is a coordination of the central double bond in the five-membered cumulene species which reduces the bond order and thus increases the bond length. This effect is missing in **6**, where no coordination was found. Additionally, organic 1,2,3-trienes can be described by two mesomeric structures: the 1,2,3-triene on one hand and a diradical displaying a central triple bond on the other hand. The relevancy of the second

(29) (a) Burlakov, V. V.; Yanovsky, A. I.; Struchkov, Y. T.; Rosenthal, U.; Spannenberg, A.; Kempe, R.; Ellert, O. G.; Shur, V. B. *J. Organomet. Chem.* **1997**, *542*, 105. (b) Thomas, D.; Peulecke, N.; Burlakov, V. V.; Baumann, W.; Spannenberg, A.; Kempe, R.; Rosenthal, U. *Eur. J. Inorg. Chem.* **1998**, 1495.

mesomer should manifest itself in **6** in an increased bond order and a conspicuous shortening of the central C–C bond. The observation of a shortened central double bond has previously been made in organic 1,2,3-trienes.³⁰

It is of interest whether the complexes **5** and **6** can be synthesized in a direct way by reacting the bisacetylides **1a** and **1b** with CO₂ in sunlight without isolating the intermediates **2a** and **2b**. Investigations into this question have so far afforded mixtures of complexes which are currently studied.

The corresponding permethyltitanocene η^2 -complex **3** (titanacyclopentadiene) inserts only one molecule of carbon dioxide under formation of the titanafuranone Cp*₂Ti[OC(=O)-C(SiMe₃)=C(C≡CSiMe₃)-] (**7**) (eq 10).



The symmetry of **7** is reduced, compared to **6**, because of the insertion of only one carbon dioxide molecule, and the NMR spectra exhibit separated resonances for the trimethylsilyl groups. The shifts of the titanafuranone are similar to those of complex **5**. Two signals at $\delta(^{13}\text{C})$ 108.5 and 120.9 ppm prove the existence of a free carbon–carbon triple bond, although their shift is found at rather low field. This might be, at least to some extent, due to the silyl substituents in the β position.

The structure resulting from the insertion of one molecule of carbon dioxide depicts a second example of a Cp*-substituted titanafuranone. A characteristically bent metallocene complex is shown. The angle between the geometrical centers of both rings and the titanium center is 141.0°. These data are in good agreement with those of formerly described titanocenes. There are some similarities to the above-mentioned complex **5** and the parent metallacycles. The distances in the metallafuranone [7: Ti–C7 2.177(2), C7–C17 1.365(3), C16–C17 1.503(4), C16–O1 1.317(3), Ti–O1 1.956(2) Å] (Figure 8) correspond very well with the data which were presented in the structural discussion of **5**. The distance of the uncoordinated triple bond [C8–C9 1.217(4) Å] is nearly identical to that found for **3** and typical for alkynylsilanes.

Complex **7** as the result of the reaction of **3** with CO₂ is as expected: One equivalent of carbon dioxide is inserted, displaying a definitely favored orientation of the insertion. More surprising is the insertion of two molecules of CO₂ into the zirconacyclocumulene **2b** to form the unprecedented nine-membered zirconacycle **6**. It initially seems obvious that the observed reactivity is a characteristic feature of the unusual cyclocumulene structure. A ready insertion of CO₂ into both metal–carbon bonds of the metallacycle would represent a plausible and very direct mechanism to produce **6**. However, it is possible to explain the formation of **6** starting from a presumed equilibrium between a η^2 - and a η^4 -permethylzirconocene complex. Then **2b** would start to react in the same manner as complex **3**, forming the zirconium analogue of **7**. While this complex is stable against further carbon dioxide insertions in the case of the smaller titanium, it seems reasonable in the case of the larger zirconium to propose a relocation of the zirconocene unit to form a seven-membered zirconacycle.

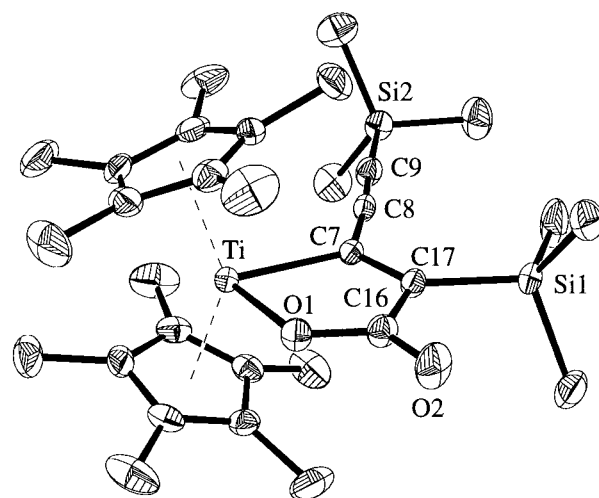
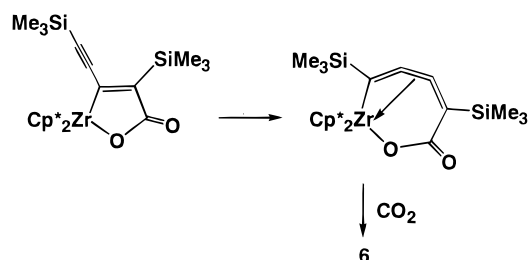


Figure 8. ORTEP diagram (30% probability) of complex **7**. Selected bond distances (Å) and angles (deg): Ti–C7 2.177(2), C7–C17 1.365(3), C16–C17 1.503(4), C16–O1 1.317(3), C16–O2 1.227(3), Ti–O1 1.956(2), C7–C8 1.417(3), C8–C9 1.217(4), C7–Ti–O1 77.75(8), Ti–C7–C17 112.4(2), C7–C17–C16 113.9(2), C17–C16–O1 114.4(2), C16–O1–Ti 121.6(2), C17–C7–C8 124.6(2), C7–C8–C9 174.7(3), C8–C9–Si2 176.8(2), C7–C17–Si1 130.5(2).

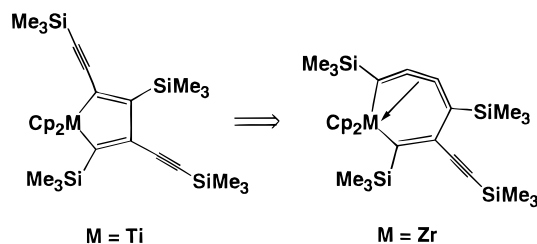
This species can undergo another insertion reaction with CO₂ to yield complex **6** (Scheme 3).

Scheme 3



In support of this view are the reaction courses found for the coupling of titanocene and zirconocene with 2 equiv of Me₃SiC≡C–C≡CSiMe₃; titanocene leads to a selective coupling resulting in the formation of a titanacyclopentadiene displaying one trimethylsilylalkynyl substituent in the α -position to the metal center.^{5k,7}

Scheme 4



The corresponding reaction of zirconocene affords a different product, as Buchwald et al. reported;^{5e} the formation of a seven-membered zirconacyclocumulene is found, which was presumed to be formed via the intermediacy of the zirconacyclopentadiene derivative analogous to the end product of the titanocene reaction (Scheme 4).

Conclusion

Due to steric reasons, the complexes Cp*₂Ti(η^2 -Me₃SiC₂-SiMe₃) and Cp*₂Zr(η^2 -Me₃SiC₂SiMe₃) do not react with

(30) (a) van den Hoek, W. G. M.; Kroon, J.; Kleijn, H.; Westmijze, H.; Vermeer, P.; Bos, H. J. T. *J. Chem. Soc., Perkin Trans. 2* **1979**, 423. (b) Higuchi, H.; Asano, K.; Ojima, J.; Yamamoto, K.; Yoshida, T.; Adachi, T.; Yamamoto, G. *J. Chem. Soc., Perkin Trans. 1* **1994**, 1453.

butadiynes $\text{RC}\equiv\text{C}-\text{C}\equiv\text{CR}$. Stable five-membered zirconacyclocumulenes $\text{Cp}^*_2\text{Zr}(\eta^4-1,2,3,4-\text{RC}_4\text{R})$, $\text{R} = \text{Ph}$ (**2a**) and SiMe_3 (**2b**) (zirconacyclopenta-2,3,4-trienes) can be synthesized by two new and well-suited methods. The first is the rearrangement of the permethylmetallocene bisacetylides $\text{Cp}^*_2\text{Zr}(\text{C}\equiv\text{CR})_2$, $\text{R} = \text{Ph}$ (**1a**), SiMe_3 (**1b**), in sunlight, and the second is the reduction of $\text{Cp}^*_2\text{ZrCl}_2$ with Mg in the presence of disubstituted butadiynes $\text{RC}\equiv\text{C}-\text{C}\equiv\text{CR}$. The first route realizes preparatively what has been predicted theoretically.^{9a}

For Cp^*_2Ti , only titanacycloprenes $\text{Cp}^*_2\text{Ti}(\eta^2-1,2-\text{Me}_3\text{-SiC}_2\text{C}\equiv\text{CSiMe}_3)$ (**3**) and C–C coupling products were obtained.

It has to be outlined that the zirconacyclocumulene **2b** and the titanacycloprenene **3** are the first examples in which the underlying substrate $\text{Me}_3\text{SiC}\equiv\text{C}-\text{C}\equiv\text{CSiMe}_3$ is not cleaved by either our titanocene or zirconocene source (not regarding coupling reactions^{5e,6,7}). It has been assumed that the special electronic effects of the trimethylsilyl group (withdrawing electron density, especially from the central C–C single bond, indicated by the extreme resonance structure $\text{Me}_3\text{Si}^{(-)}=\text{C}=\text{C}^{(+)}-\text{C}^{(+)}=\text{C}=\text{Si}^{(-)}\text{Me}_3$, and thus preparing for a further activation) is responsible for the observation that cumulenes and other complexed compounds have never been found employing this substrate. The simple use of the pentamethylcyclopentadienyl ligand instead of the unsubstituted cyclopentadienyl linkage restricts this reasoning as it obviously does prevent the cleavage and makes possible the formation of two complexes with intact C_4 backbones. A comparison of **2b** and **3** focuses on the influence of the metals. The larger zirconium generates the η^4 -complex, while the smaller titanium evidently is too small to encompass all four diyne carbons in its coordination sphere.

The existence of a metallacyclocumulene structure (η^4 -butadiyne complex) seems to mainly depend on steric factors resulting from the metals and the substituents of the butadiyne as well as from the Cp^* ligands. Compared to $\text{Cp}_2\text{Ti}(\eta^4-1,2,3,4-\text{PhC}_4\text{Ph})$, the complex $\text{Cp}^*_2\text{Zr}(\eta^4-1,2,3,4-\text{PhC}_4\text{Ph})$ **2a** is much more stable in solution. The metallacyclocumulene $\text{Cp}^*_2\text{Zr}(\eta^4-1,2,3,4-\text{Me}_3\text{SiC}_4\text{SiMe}_3)$ **2b** is stable, whereas all other attempts failed to prepare metallacyclocumulenes starting from $\text{Me}_3\text{SiC}\equiv\text{C}-\text{C}\equiv\text{CSiMe}_3$ and “ Cp_2Ti ” or “ Cp_2Zr ”. The conclusion is that Cp^* ligands stabilize such unusual five-membered metallacyclocumulenes only for zirconium.

Experimental Section

All operations were carried out under an inert atmosphere (argon) using standard Schlenk techniques. Prior to use, solvents were freshly distilled from sodium tetraethylaluminate under argon. Deuterated solvents were treated with sodium or sodium tetraethylaluminate, distilled, and stored under argon. NMR: Bruker ARX 400 at 9.4 T (chemical shifts given in ppm relative to TMS), recorded at ambient temperature, unless otherwise noted. Melting points were measured in sealed capillaries on a Büchi 535 apparatus. Elemental analyses: Leco CHNS-932 elemental analyzer. Infrared spectra were recorded with a Nicolet Magna 550 (Nujol mulls using KBr plates). Mass spectrometer: AMD 402.

$\text{Cp}^*_2\text{Zr}(\text{C}\equiv\text{CR})_2$, $\text{R} = \text{Ph}$ (1a**), SiMe_3 (**1b**).** About 3–5 mmol of the alkyne $\text{HC}\equiv\text{CR}$ was dissolved in 5 mL of toluene, cooled to -78°C , and 1 equiv of *n*-butyllithium (2.5 M/hexane) was added. After warming up to room temperature, 0.5 equiv of the complex $\text{Cp}^*_2\text{ZrCl}_2$ was added and the solution was stirred for 24 h, the solvents were then distilled in vacuo, and the residue was suspended in 10 mL of *n*-hexane. After filtration and crystallization at -78°C , the mother liquor was decanted and the crystals were dried in vacuo.

$\mathbf{1a}$ ($\text{R} = \text{Ph}$). Amounts of 316 mg (3.10 mmol) of $\text{PhC}\equiv\text{CH}$ and 650 mg (1.50 mmol) of $\text{Cp}^*_2\text{ZrCl}_2$ give 185 mg (22%) of **1a**; mp $219-223^\circ\text{C}$ (dec under argon). Anal. Calcd for $\text{C}_{36}\text{H}_{40}\text{Zr}$ (563.9): C, 76.67; H, 7.15. Found: C, 76.61; H, 7.28. ^1H NMR (THF- d_8) δ /ppm: 2.11

(s, 30H, C_5Me_5), 7.35 (m, 4H, *o*-Ph), 7.22 (m, 4H, *m*-Ph), 7.15 (m, 2H, *p*-Ph). ^{13}C NMR (THF- d_8) δ /ppm: 12.5 (C_5Me_5), 118.3 ((C- β), 121.0 (C_5Me_5), 127.1 (*i*-Ph), 127.2 (*p*-Ph), 128.7 (*m*-Ph), 131.8 (*o*-Ph), 153.0 (C- α). MS (70 eV) m/z : 562 (M^+), 361 (Cp^*_2Zr^+), 204 ($\text{PhC}_2-\text{C}_2\text{Ph}^+$). IR (Nujol, cm^{-1}): 2073 m, 1593 w, 1493 vs, 1202 s, 1068 w, 1025 m, 785 m, 758 vs, 691 s, 541 s.

$\mathbf{1b}$ ($\text{R} = \text{SiMe}_3$). Amounts of 432 mg (4.40 mmol) of $\text{Me}_3\text{SiC}\equiv\text{CH}$ and 950 mg (2.20 mmol) of $\text{Cp}^*_2\text{ZrCl}_2$ afford 450 mg (37%) of **1b**; mp $162-166^\circ\text{C}$ (dec under argon). Anal. Calcd for $\text{C}_{30}\text{H}_{48}\text{Si}_2\text{Zr}$ (556.1): C, 64.80; H, 8.70. Found: C, 64.82; H, 8.87. ^1H NMR (C_6D_6) δ /ppm: 0.24 (s, 18H, SiMe_3), 2.01 (s, 30H, C_5Me_5). ^{13}C NMR (C_6D_6) δ /ppm: 0.6 (SiMe_3), 12.6 (C_5Me_5), 120.6 (C_5Me_5), 122.3 (C- β), 175.0 (C- α). MS (70 eV) m/z : 554 (M^+), 360 (Cp^*_2Zr^+). IR (Nujol, cm^{-1}): 2027 m, 1424 s, 1244 vs, 1025 m, 855 vs, 837 vs, 757 m, 683 vs, 604 s.

$\text{Cp}^*_2\text{Zr}(\eta^4-1,2,3,4-\text{PhC}_4\text{Ph})$ (2a**).** (a) To an amount of 1420 mg (3.28 mmol) of $\text{Cp}^*_2\text{ZrCl}_2$ and 80 mg (3.29 mmol) of Mg turnings was added a solution of 664 mg (3.28 mmol) of 1,4-diphenylbutadiyne in 20 mL of THF. The mixture was stirred for 24 h at $55-60^\circ\text{C}$, and the color of the solution changed from light yellow to yellow-red. The warm solution was filtered, concentrated to 10 mL and allowed to stand at room temperature to induce the precipitation of red crystals which were separated, washed with cold *n*-hexane (-75°C), and dried in vacuo to give 834 mg (45%) of **2a**. (b) An amount of 150 mg (0.23 mmol) of $\text{Cp}^*_2\text{Zr}(\text{C}\equiv\text{CPh})_2$ **1a** was dissolved in 5 mL of toluene. The solution was allowed to stand in sunlight for 4 days, and the color of the solution turned from light yellow to red. The solvent was removed under vacuum, and the red residue was dissolved in 1 mL of *n*-hexane. At -78°C , red crystals appeared which were separated, washed with cold *n*-hexane (-75°C), and dried in vacuo to give 95 mg (74%) of **2a**; mp $226-228^\circ\text{C}$ (dec under argon). Anal. Calcd for $\text{C}_{36}\text{H}_{40}\text{Zr}$ (563.93): C, 76.67; H, 7.15. Found: C, 76.78; H, 7.15. ^1H NMR (THF- d_8) δ /ppm: 1.66 (s, 30H, C_5Me_5), 7.25 (2H, *p*-Ph), 7.41 (4H, *m*-Ph), 7.88 (4H, *o*-Ph). ^{13}C NMR (THF- d_8) δ /ppm: 11.9 (C_5Me_5), 113.7 (C_5Me_5), 118.4 (C- β), 128.2 (*p*-Ph), 129.0 (*m*-Ph), 134.4 (*o*-Ph), 136.7 (*i*-Ph), 179.4 (C- α). MS (70 eV) m/z : 563 (M^+), 361 (Cp^*_2Zr^+), 202 ($\text{PhC}_2-\text{C}_2-\text{Ph}^+$).

$\text{Cp}^*_2\text{Zr}(\eta^4-1,2,3,4-\text{Me}_3\text{SiC}_4\text{SiMe}_3)$ (2b**).** (a) An amount of 292 mg (1.50 mmol) of 1,4-bis(trimethylsilyl)butadiyne was dissolved in 10 mL of THF. The solution was added to 650 mg (1.50 mmol) of $\text{Cp}^*_2\text{ZrCl}_2$ and 36 mg (1.50 mmol) of Mg turnings. The mixture was kept at $55-60^\circ\text{C}$ and stirred for 48 h. The color of the solution changed from light yellow to orange-red. The solution was then filtered, and the solvent was removed in vacuo. The residue was extracted three times with 5 mL portions of *n*-hexane. After filtration, concentration of the clear solution to about 5 mL, and crystallization at -78°C , an amount of 669 mg (80%) of **2b** formed which was filtered and dried in vacuo to give orange-red crystals. (b) An amount of 135 mg (0.24 mmol) of $\text{Cp}^*_2\text{Zr}(\text{C}\equiv\text{CSiMe}_3)_2$ **1b** was dissolved in 5 mL of toluene under argon. After standing for 4 days in sunlight, the color of the solution turned from light yellow to red. The solvent was removed in vacuo, and the red residue was redissolved in 1 mL of *n*-hexane. While the solution was standing at -78°C , red crystals appeared which were separated, washed with cold *n*-hexane (-75°C), and dried in vacuo to give 101 mg (79%) of **2b**; mp 195°C (dec under argon). Anal. Calcd for $\text{C}_{30}\text{H}_{48}\text{Si}_2\text{Zr}$ (556.1): C, 64.80; H, 8.70. Found: C, 64.57; H, 8.64. ^1H NMR (THF- d_8) δ /ppm: 0.45 (s, 18H, SiMe_3), 1.61 (s, 30H, C_5Me_5). ^{13}C NMR (THF- d_8) δ /ppm: 3.2 (SiMe_3), 12.1 (C_5Me_5), 113.4 (C_5Me_5), 144.5 (C- β), 188.0 (C- α). MS (70 eV) m/z : 556 (M^+), 360 (Cp^*_2Zr^+).

$\text{Cp}^*_2\text{Ti}(\eta^2-1,2-\text{Me}_3\text{SiC}_2\text{C}\equiv\text{CSiMe}_3)$ (3**).** A suspension of 1045 mg (2.68 mmol) of $\text{Cp}^*_2\text{TiCl}_2$, 66 mg (2.71 mmol) of Mg turnings, and 521 mg (2.68 mmol) of 1,4-bis(trimethylsilyl)butadiyne in 15 mL of THF was stirred for 8 h at $55-60^\circ\text{C}$. The resulting green solution was evaporated to dryness in vacuo, and the residue was extracted with 25 mL of *n*-hexane. After standing at -78°C for 2 days, red crystals appeared which were separated, washed with cold *n*-hexane (-75°C), and dried in vacuo to give 1193 mg (87%) of **3**; mp $141-142^\circ\text{C}$ (dec under argon). Anal. Calcd for $\text{C}_{30}\text{H}_{48}\text{Si}_2\text{Ti}$ (512.8): C, 70.27; H, 9.44. Found: C, 70.34; H, 9.69. ^1H NMR (toluene- d_8 , 188 K) δ /ppm: 0.21 (s, 9H, SiMe_3), 0.27 (s, 9H, SiMe_3), 1.66 (s, 15H, C_5Me_5). ^{13}C NMR

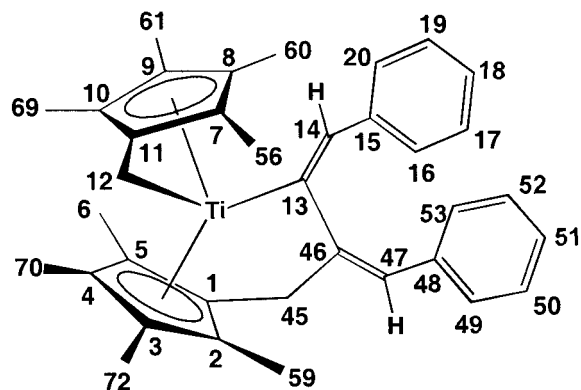


Figure 9. Molecular structure of **4** labelled according to the labelling of the respective crystal structure. The labels are used for the assignment of the NMR signals.

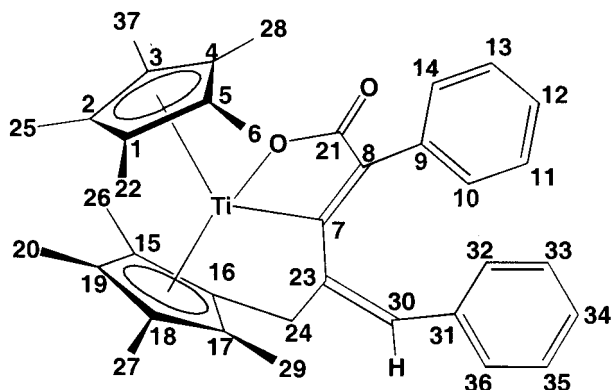


Figure 10. Molecular structure of **5** labelled according to the labelling of the respective crystal structure. The labels are used for the assignment of the NMR signals.

(toluene-*d*₈, 188 K) δ /ppm: 0.4 (SiMe₃), 2.4 (SiMe₃), 11.9 (C₅Me₅), 105.1, 110.7 (C≡C), 121.3 (C₅Me₅), 205.3 (C-β), 227.5 (coord. C≡C). MS (70 eV) *m/z*: 512 (M⁺). IR (Nujol, cm⁻¹): 2092 (ν(C≡C)), 1608 (ν(C≡C) coord.).

[η⁵-C₅Me₄-(CH₂)₂]-Ti[*-C(=CHPh)C(=CHPh)CH₂-η⁵-C₅Me₄] (**4**). A suspension of 1066 mg (2.74 mmol) of Cp*₂TiCl₂, 67 mg (2.76 mmol) of Mg turnings, and 559 mg (2.76 mmol) of 1,4-diphenylbutadiyne in 20 mL of THF was stirred for 8 h at 55–60 °C.*

The volatile material was removed under vacuum, and the residue was dissolved in 60 mL of *n*-hexane at 60 °C. The warm solution was filtered and evaporated under vacuum to give 1181 mg (76%) of a green solid. Subsequent recrystallization from *n*-hexane produced dark-green crystals; mp 158–160 °C (dec under argon) (Figure 9). Anal. Calcd for C₃₆H₄₀Ti (520.6): C, 83.06; H, 7.74. Found: C, 82.99; H, 7.86. ¹H NMR (C₆D₆) δ /ppm: 0.96 (s, 3H, C61), 1.13 (s, 3H, C56), 1.26 (s, 3H, C60), 1.37 (s, 3H, C72), 1.49 (s, 3H, C70), 1.66 (d, 1H, C12), 1.71 (s, 3H, C59), 1.97 (s, 3H, C6), 2.21 (d, 1H, C12), 2.33 (s, 3H, C69), 3.22 (d, 1H, C45), 3.72 (dd, 1H, C45), 4.87 (s, 1H, C14), 5.62 (d, 1H, C47), 6.91 (t, 1H, C51), 6.98 (t, 1H, C18), 7.03 (t, 2H, C50/52), 7.15 (t, 2H, C17/19), 7.37 (d, 2H, C49/53), 7.63 (d, 2H, C16/20). ¹³C NMR (C₆D₆) δ /ppm: 9.5 (C59), 10.2 (C61), 10.2 (C56), 10.3 (C60), 10.7 (C72), 11.5 (C70), 13.5 (C6), 16.5 (C69), 33.4 (C45), 79.5 (C12), 113.2 (C2), 113.2 (C47), 114.6 (C4), 119.5 (C3), 120.6 (C5), 122.1 (C14), 122.6 (C8), 125.6 (C51), 126.2 (C7), 126.2 (C18), 128.1 (C16/20), 128.2 (C50/52), 128.3 (C11), 128.5 (C49/53), 128.7 (C9), 129.0 (C17/19), 129.4 (C10), 130.5 (C1), 139.0 (C15), 139.8 (C48), 147.5 (C46), 208.0 (C13). MS (70 eV) *m/z*: 521 (M⁺).

Cp*Ti[*-OC(=O)C(Ph)C(=C(=CHPh)CH₂-η⁵-C₅Me₄]* (**5**). An amount of 155 mg (0.298 mmol) of **4** was dissolved in 10 mL of *n*-hexane under argon. The resulting green solution was filtered, argon was carefully removed from the flask under vacuum, and the flask containing the solution was charged with carbon dioxide. After 3 days at room temperature, dark red crystals had formed, which were separated, washed with *n*-hexane, and dried in vacuo to give 125 mg (74%); mp 239–241 °C (Figure 10). Anal. Calcd for C₃₇H₄₀O₂Ti (564.60): C, 78.71; H, 7.14. Found: C, 78.95; H, 7.24. ¹H NMR (C₆D₆) δ /ppm: 1.18 (s, 3H, C20), 1.43 (s, 3H, C29), 1.76 (s, 15H, C6/22/25/28/37), 1.91 (s, 3H, C27), 2.02 (s, 3H, C26), 2.72 (dd, 1H, C24), 3.90 (dd, 1H, C24), 5.40 (d, 1H, C30), 6.89 (t, 1H, C34), 7.02 (t, 2H, C33/35), 7.06 (t, 1H, C12), 7.07 (d, 2H, C32/36), 7.32 (t, 2H, C11/13), 8.17 (d, 2H, C10/14). ¹³C NMR (C₆D₆) δ /ppm: 10.1 (C29), 10.4 (C20), 11.4 (C27), 11.9 (C6/22/25/28/37), 12.5 (C26), 33.9 (C24), 113.9 (C30), 118.1 (C15), 122.3 (C16), 122.7 (C17), 126.2 (C1/2/3/4/5), 126.4 (C34), 126.6 (C12), 128.1 (C33/35), 128.2 (C11/13), 128.7 (C32/36), 128.8 (C10/14), 129.7 (C18), 133.0 (C19), 138.1 (C9 or C31), 139.8 (C8), 140.4 (C9 or C31), 148.2 (C23), 165.2 (C21), 224.4 (C7). MS (70 eV) *m/z*: 564 (M⁺), 520 (M⁺ - CO₂), 318 (Cp*₂Ti⁺). IR (Nujol, cm⁻¹): 1635 ν(C=O).

Cp*₂Zr[*-OC(=O)C(SiMe₃)=C=C=C(SiMe₃)C(=O)O-*] (**6**). An amount of 161 mg (0.29 mmol) of **2b** was dissolved in 7 mL of THF. The solution was stirred for 3 h under an atmosphere of CO₂ at room temperature. The solvent was removed, and the residue was extracted three times with portions of 3 mL of *n*-hexane. Cooling for 48 h at -78 °C afforded 97 mg (52%) of yellow crystals which were separated

Table 2. Crystallographic Data of the Complexes

	2a	2b	3	4	5	6	7
cryst. color, habit	orange, prism	orange, prism	red, prism	green, prism	orange, prism	yellow, prism	red, prism
cryst. system	monoclinic	monoclinic	triclinic	monoclinic	monoclinic	orthorhombic	triclinic
space group	C2/c	P2 ₁ /c	P-1	P2 ₁ /c	P2 ₁ /n	Fddd	P-1
lattice constants							
<i>a</i> (Å)	27.086(5)	10.595(2)	11.237(2)	26.632(5)	17.064(3)	17.104(3)	10.567(2)
<i>b</i> (Å)	15.533(3)	18.220(4)	11.534(2)	8.931(2)	8.838(2)	17.173(3)	12.213(2)
<i>c</i> (Å)	14.207(3)	15.891(3)	13.691(3)	25.953(5)	21.308(4)	48.170(10)	13.991(3)
α (deg)			76.36(3)				92.07(3)
β (deg)	104.31(3)	94.50(3)	67.09(3)	109.16(3)	107.70(3)		100.15(3)
γ (deg)			74.46(3)				114.87(3)
<i>Z</i>	8	4	2	8	4	16	2
cell volume	5792(2)	3058.2(11)	1557.3(5)	5831(2)	3061.4(10)	14149(5)	1600.2(5)
density (g/cm ⁻³)	1.293	1.208	1.093	1.186	1.225	1.209	1.156
temp (K)	293(2)	200(2)	200(2)	293(2)	293(2)	293(2)	293(2)
μ (Mo K α) (mm ⁻¹)	0.402	0.453	0.367	0.315	0.310	0.409	0.366
θ range (deg)	1.99–24.22	2.23–24.23	1.85–24.27	1.59–21.05	1.83–21.05	1.73–24.33	1.85–24.15
no. of rflns (measd)	12691	8957	4643	11175	5945	10158	4733
no. of rflns (indep)	4581	4579	4643	6155	3145	2828	4733
no. of rflns (obsd)	2814	3595	3685	3793	1669	2275	3888
no. of parameters	334	288	298	667	361	177	325
R1 (<i>I</i> > 2 σ (<i>I</i>))	0.033	0.049	0.044	0.046	0.045	0.035	0.040
wR2 (all data)	0.080	0.135	0.136	0.111	0.100	0.093	0.127

from the mother liquor by filtration and dried in vacuo; mp 196–198 °C. Anal. Calcd for $C_{32}H_{48}O_4Si_2Zr$ (644.26): C, 59.67; H, 7.51. Found: C, 59.54; H, 7.37. 1H NMR (THF- d_8) δ /ppm: 0.20 (s, 18H, $SiMe_3$), 1.90 (s, 15H, C_5Me_5). ^{13}C NMR (THF- d_8) δ /ppm: -1.2 ($SiMe_3$), 10.9 (C_5Me_5), 123.3 (C_5Me_5), 134.4 ($C=C$), 167.8 (CO), 185.9 ($C=C$). MS (70 eV) m/z : 642 (M^+), 598 ($M^+ - CO_2$), 525 ($M^+ - CO_2 - SiMe_3$), 360 ($Cp^*_2Zr^+$). IR (Nujol, cm^{-1}): 2096 w, 1928 w, 1636 m, 1414 s, 1261 s, 1023 s, 841 vs.

$Cp^*_2Ti[-OC(=O)C(SiMe_3)=C(C\equiv CSiMe_3)-]$ (7). An amount of 100 mg (0.20 mmol) of **3** was dissolved in 5 mL of THF and stirred for 2 h under an atmosphere of CO_2 at room temperature. The solvent was removed, and the red residue was redissolved in 2 mL of THF. Cooling for 24 h at -78 °C yielded 90 mg (82%) of a red-brown crystalline product which was separated from the mother liquor by filtration and dried in vacuo; mp 208 °C. Anal. Calcd for $C_{31}H_{48}O_2Si_2Ti$ (556.77): C, 66.87; H, 8.68. Found: C, 67.03; H, 8.72. 1H NMR (C_6D_6) δ /ppm: 0.18 (s, 9H, $SiMe_3$), 0.70 (s, 9H, $SiMe_3$), 1.76 (s, 15H, C_5Me_5). ^{13}C NMR (C_6D_6) δ /ppm: -0.2 ($SiMe_3$), 1.1 ($SiMe_3$), 12.0 (C_5Me_5), 108.5, 120.9 ($C\equiv C$), 125.8 (C_5Me_5), 167.1, 163.8 (CO, $C-\beta$), 221.1 ($C-\alpha$). MS (70 eV) m/z : 556 (M^+), 541 ($M^+ - Me$), 513 ($M^+ - Me - C_2H_4$), 426 ($M^+ - C_5H_9O_2Si$), 318 ($Cp^*_2Ti^+$). IR (Nujol,

cm^{-1}): 2095 m, 2076 m, 1627 vs, 1491 m, 1233 s, 1022 m, 853 vs, 837 vs.

X-ray Crystallographic Study of Complexes. Data were collected with a STOE-IPDS diffractometer using graphite-monochromated Mo $K\alpha$ radiation. The structures were solved by direct methods (SHELXS-86)³¹ and refined by full-matrix least-squares techniques against F^2 (SHELXL-93).³² The hydrogen atoms were included at calculated positions. All other nonhydrogen atoms were refined anisotropically. Cell constants and other experimental details were collected and recorded in Table 2. XP (SIEMENS Analytical X-ray Instruments, Inc.) was used for structure representations and for calculating certain additional angles and distances in the determined structures.

Supporting Information Available: Tables of crystal data, structure solution and refinement, atomic coordinates, bond lengths and angles, and anisotropic thermal parameters for **2a**, **2b**, **3**, **4**, **5**, **6**, and **7** (PDF). An X-ray crystallographic file, in CIF format, is also available. This material is available free of charge via the Internet at <http://pubs.acs.org>.

JA991046Z

(31) Sheldrick, G. M. *Acta Crystallogr.* **1990**, *A46*, 467.

(32) Sheldrick, G. M. *SHELXL-93*; University of Göttingen: Göttingen, Germany, 1993.